Relativistic quantum mechanical calculations of electron-impact broadening for spectral lines in Be-like ions

B. Duan[1], M. A. Bari[2], Z. Q. Wu[1], Y. Jun[1,3], Y. M. Li[1], and J. G. Wang[1]

[1] Data Center for High Energy Density Physics, Institute of Applied Physics and Computation Mathematics, 100088 Beijing, PR China
e-mail: alexduan1967@hotmail.com, duan_bin@iapcm.ac.cn
[2] Pakistan Atomic Energy Commission, PO Box 1114, 44000 Islamabad, Pakistan
[3] HEDPS, Center for Applied Physics and Technology, Peking University, 100871 Beijing, PR China

ABSTRACT

Aims. We present relativistic quantum mechanical calculations of electron-impact broadening of the singlet and triplet transition 2s3s ← 2s3p in four Be-like ions from N IV to Ne VII.
Methods. In our theoretical calculations, the **K**-matrix and related symmetry information determined by the colliding systems are generated by the DARC codes.
Results. A careful comparison between our calculations and experimental results shows good agreement. Our calculated widths of spectral lines also agree with earlier theoretical results. Our investigations provide new methods of calculating electron-impact broadening parameters for plasma diagnostics.

Key words. line: profiles – atomic processes – atomic data

1. Introduction

Generally, radiation damping of an excited atom leads to broadening of spectral lines. In dense plasmas, radiation damping stems from the interactions of an emitting atom or ion with perturbing plasma constituents. Among these interactions, the electron colliding with ions can lead to excitations and broadening of ionic spectral lines. The electron-impact broadening is a major contributor to radiative acceleration in stellar interiors and is of particular importance as a diagnostic tool in high-temperature plasmas. Not only is it important to precision spectroscopy, but also reveals dependence on major plasma characteristics, such as density and temperature. In the case of plasma diagnostics, the careful analysis of line profiles is a powerful technique for studying atomic and molecular interactions. The knowledge of electron-impact broadening is paramount for probing matter under extreme physical conditions such as in stellar atmospheres. In stellar interiors, electron-impact broadening contributes significantly to radiative acceleration, because of high electron density, and is imperative for evolutionary models, atomic abundances, and radiative opacity calculations.

To study electron-impact broadening, several theoretical methods and techniques have been used in the literature (Griem 1974; Dimitrijević & Konjević 1980). However, there have been very few quantum mechanical calculations of electron-impact broadening and shift in spectral lines. Recently, the full quantum mechanical calculations for electron impact broadening of the 2s3s−2s3p transitions for the four Be-like ions from N IV to Ne VII have been performed by Elabidi et al. (2008). These calculations are based on the nonrelativistic quantum mechanics and intermediate coupling. In the context of quantum mechanics, electron-impact broadening and shift of spectral lines is studied by two different methods, i.e., calculating the scattering cross sections and generating the **K**-matrix. In the present work, we adopt the latter approach, defined by calculating **K**-matrix, which is similar to the method adopted by Seaton (1987).

The main aim of this paper is to perform quantum mechanical calculations of electron-impact broadening of the transition 2s3s ← 2s3p in Be-like ions, i.e., N IV, O V, F VI, and Ne VII. We also report new electron-impact broadening parameters for transitions in Be-like ions. We employ the impact approximation theory to obtain line broadening and shift parameters at various plasma conditions. In our numerical computations, Dirac Atomic R-matrix Codes (DARC) and General Purpose Relativistic Atomic Structure Package (GRASP0-10.10; Norrington 2009) are used to solve $(N + 1)$-electron colliding systems so that the scattering matrices (reactance matrices) are obtained. The paper is organized as follows. Section 2 gives details of the methods used to calculate electron-impact broadening parameters. It also outlines the impact approximation and scattering matrix theory. Section 3 explains our strategy for constructing the atomic structure of each ion and selection of configurations. The comparison between experimental and theoretical data, accuracy of our results, final selected data of spectral line widths, the content and organization of the delivered tables are described in Sect. 4. Our conclusions are given in Sect. 5.

2. Theory and methods

2.1. Impact approximation theory

In dense plasmas, spectral line broadening arises from perturbations by the constituents of the plasma (both ions and electrons).

Ions have large masses than electron and always move much slowly, so in evaluating line broadening parameters it is often a good approximation to treat them as being stationary. The effect of stationary ions is equal to an average ion microfield, introduced by Hooper (1966). This microfield perturbs the radiating ions by Stark effect and leads to spectral line broadening, known as Stark broadening. Similarly, the high-speed electrons also perturb the emitting ions through collisions, and cause the interruption of spontaneous emission. This interruption will broaden the widths of emission lines, and is known as electron-impact broadening. The radiative transition of spontaneous emission between upper (X_b) and lower state (X_a) of radiating ion is written as:

$$X_b \rightarrow X_a + \hbar\omega. \tag{1}$$

The impact approximation theory was first formulated by Baranger (1958a−c) and later reviewed by Griem (1974). The theory considers a single binary collision between the perturber and the perturbed ion. During the time of electron collision with a radiating ion, the interaction between perturbing ions is ignored, and at a time each electron interacts only with one perturbed ion. Within impact approximation and the isolated line approximation, the line profile is Lorentzian, i.e.,

$$\phi_\omega = \frac{w}{\pi} \frac{1}{(\omega - d - \omega_0)^2 + w^2}. \tag{2}$$

Where ω_0 is the central line frequency, d is the shift, and $2w$ is the spectral line full width at half maximum. The width and shift of a spectral line are linearly proportional to electron density N_e and depend on the scattering matrix $\mathbf{S}$ for binary collisions. The final expression relating the shift and width of a spectral line could be obtained by averaging over Maxwell distribution of electron velocities. A simplified and compact expression has independently also been derived by Elabidi et al. 2004 in intermediate coupling scheme:

$$w + \mathrm{i}d = \alpha N_e \int_0^\infty T_e^{-3/2} \exp(-\varepsilon/T)\Omega(\varepsilon)\mathrm{d}\varepsilon. \tag{3}$$

Where parameter $\alpha = 2.8674 \times 10^{-23}$ eV cm^3. The units of electron density N_e is cm^{-3}. Electron temperature T_e and colliding electron energy ε are in Rydberg, and spectral line width w and shift d are in eV. The electron collision strength $\Omega(\varepsilon)$ in jj coupling is defined by Peach (1996) (if intermediate coupling is considered, $\Omega(\varepsilon)$ can be found in the works of Elabidi et al. 2004; or Elabidi et al. 2008), i.e.,

$$\Omega(\varepsilon) = \sum_{J_i^T J_f^T j j' \ell \ell'} (-1)^{J_i + J_f + 2J_f^T + j + j'} \frac{1}{2}\left(2J_i^T + 1\right)$$

$$\times \left(2J_f^T + 1\right) \begin{Bmatrix} J_f^T & J_i^T & 1 \\ J_i & J_f & j \end{Bmatrix} \begin{Bmatrix} J_f^T & J_i^T & 1 \\ J_{i'} & J_{f'} & j' \end{Bmatrix}$$

$$\times \frac{1}{2}\left[\delta_{\ell\ell'}\delta_{jj'}\delta_{J_iJ_{i'}}\delta_{J_fJ_{f'}} - \mathbf{S}_I\left(J_{i'}\,\ell'\,j'\,J_i^T, J_i\ell jJ_i^T\right)\right.$$

$$\left. \times \mathbf{S}_F^*\left(J_{f'}\,\ell'\,j'\,J_f^T, J_f\ell jJ_f^T\right)\right]. \tag{4}$$

Where two {...} are the "6j" symbols. The upper and lower states of the transition are represented by the total angular momentum states $|J_iM_i\rangle$ and $|J_fM_f\rangle$ respectively, and $\mathbf{S}_I(J_{i'}\,\ell'\,j'\,J_i^T, J_i\ell jJ_i^T)$ is a scattering matrix element corresponding to an colliding electron scattered by the upper state X_b

$$X_b + e(\varepsilon, \ell, j) \rightarrow X_b + e\left(\varepsilon, \ell', j'\right). \tag{5}$$

Where ℓ, ℓ' and j, j' are the orbital and total angular momentum of colliding electrons before and after the collision with the target ion X_b respectively. During the colliding process, the total energy $E_I = E_b + \varepsilon = E_a + \varepsilon + \omega$, total parity Π, total spin angular momentum S^T and total angular momentum J_i^T of ($N + 1$)-electron colliding system are conserved. The $\mathbf{S}_F^*(J_{f'}\,\ell'\,j'\,J_f^T, J_f\ell jJ_f^T)$ is the conjugate matrix of a scattering matrix $\mathbf{S}$ corresponding to colliding process of the lower state X_a

$$X_a + e(\varepsilon, \ell, j) \rightarrow X_a + e\left(\varepsilon, \ell', j'\right). \tag{6}$$

In Eq. (6), the total energy $E_F = E_a + \varepsilon$, parity Π, total spin angular momentum S^T and total angular momentum J_f^T of ($N + 1$)-electron colliding system are conserved. The above two scattering processes, described in Eqs. (5) and (6) will share the same total spin angular momentum S^T and opposite parity Π when only electric dipole transition is considered. This information is useful for the later numerical calculations.

2.2. Scattering matrix

The calculation of scattering matrices S_I and S_F is necessary to obtain electron collision strength $\Omega(\varepsilon)$. These two matrices are closely related to collision processes by Eqs. (5) and (6), which are ($N + 1$)-electron colliding systems. Generally, a colliding system is constructed from N-electron target states $\Phi_i = |J_iM_i\rangle$ (possibly including pseudo states) and single particle wavefunctions $\phi_{ij} = |jm\rangle$ of the continuum electron. A state of such colliding system is well defined by the wavefunction in Berrington (1977) and Norrington (2009)

$$\Psi_k = \sum_{ij} c_{ijk}\mathfrak{I}\left[\Phi_i, \phi_{ij}\right] + \sum_m d_{mk}\theta_m. \tag{7}$$

Where $\mathfrak{I}$ is an antisymmetric operator to account for the electron exchange, j is the continuum basis function index for a particular κ value ($\kappa = -\ell - 1$, if $\kappa < 0$, else $\kappa = \ell$), and θ_m is a capture state in which all of the ($N + 1$)-electrons are bound.

The ($N + 1$)-electron colliding system, defined by Eqs. (5) or (6), is solved by using DARC to obtain a reactance $\mathbf{K}$-matrix which is real symmetric matrix. With $\mathbf{K}$-matrix, scattering matrix $\mathbf{S}$ is defined as:

$$\mathbf{S} = \frac{1 + \mathrm{i}\mathbf{K}}{1 - \mathrm{i}\mathbf{K}}. \tag{8}$$

From Eq. (8), $\mathbf{S}$ is an unitary matrix, and its real part and imaginary part are written out as

$$\mathrm{Re}\,\mathbf{S} = \frac{1 - \mathbf{K}^2}{(1 + \mathbf{K}^2)}. \tag{9a}$$

$$\mathrm{Im}\,\mathbf{S} = \frac{2\mathbf{K}}{(1 + \mathbf{K}^2)}. \tag{9b}$$

These two expressions are directly used in our numerical calculations.

3. Numerical calculations in detail

To obtain electron collision strength $\Omega(\varepsilon)$, we solved the colliding system which consists of an N-electron target ion and a colliding electron. The states of an N-electron target in DARC calculations are prepared first by a fully relativistic atomic structure code called GRASP0-10.10 as explained in the next section.

3.1. Atomic structure

In our calculations, the atomic structure data of four Be-like ions from N IV to Ne VII are obtained by using the multi-configuration Dirac-Fock (MCDF) atomic structure program GRASP0-10.10 developed by Dyall et al. (1989) and Parpia et al. (1996) included in DARC. The original GRASP0-10.10 have been partly improved by us according to our previous works (Duan et al. 2008; Bari et al. 2011) so that all the following atomic structure data can be calculated by extended average-level (EAL) mode. To calculate the atomic structure of the four Be-like ions, i.e., N IV, O V, F VI and Ne VII, we have selected the following electronic configurations: $1s^2 2s^2$, $1s^2 2s2p$, $1s^2 2s3s$, $1s^2 2s3p$, $1s^2 2s3d$, $1s^2 2s4s$, $1s^2 2s4p$, $1s^2 2s5s$, and $1s^2 2s5p$. With the selection of these configurations, it is easy to obtain the electronic orbitals, the energy levels and states of target ions. These atomic data are incorporated as input in solving $(N + 1)$-electron colliding system by DARC.

3.2. From **K** to **S**

With the atomic structure data of target ions, the $(N+1)$-electron colliding systems of Eqs. (5) and (6) are solved by DARC, and their **K** matrices and quantum numbers of angular momentum are also obtained. Then **K** matrix is used to calculate the real and imaginary parts of scattering matrix **S** with Eqs. (9). The transformation from **K** to **S** is performed by a code developed by us.

4. Numerical results and discussion

In this paper, the electron-impact broadening widths of the transition arising from the 2s3s ← 2s3p configuration in Be-like ions N IV, O V, F VI and Ne VII are calculated. In these calculations, we have used the GRASP0-10.10 package included in DARC to provide the fine-structure wavefunctions, energy levels, wavelengths, and transition rates. We obtained the electron impact collision strengths by DARC. For those configurations, each target ion has 27 bound states. All of these target states are selected as target basis in our calculations. To generate and construct the $(N + 1)$-electron colliding systems defined in Eqs. (5) and (6), two parameters of the colliding electron are defined by specific boundary limits i.e., the quantum number of orbital angular momentum is $\ell \leq 10$ and the total number of continuum basis function for a given κ is 14. The electron collision strength $\Omega(\varepsilon)$ defined in Eq. (4) is a function of colliding electron energy ε and is computed in an increasing energy sequence with an energy step of $\Delta\varepsilon = 0.02$ Rydberg by the same procedure. To realize and confirm our numerical calculations, it is necessary for us to study the convergence of collision strength $\Omega(\varepsilon)$ with both the orbital angular momentum ℓ and the colliding electron energy ε. In Fig. 1 the maximum ℓ of the colliding electron in Eq. (4) is limited by 10 or 15, and $\Omega(\varepsilon)$ are present as a function ε in transition $^3S_1 \leftarrow {}^3P_1$ in N IV ion. It can be seen that $\Omega(\varepsilon)$ converges with the orbital angular momentum ℓ if ℓ is large enough, and that it also decreases with the colliding electron energy ε. Thus the electron impact broadening in Eq. (3) is numerically calculated by the trapezoidal integration technique. The full width at half maximum (*FWHM* $W = 2w$) for transitions 2s3s ← 2s3p for various electron temperature T_e and electron density N_e are given in Tables 1–7. The full quantum mechanical calculations of line widths w_2 and its simplified calculations w_1 by Elabidi et al. (2008) are also listed in Tables 1–7 for comparison purposes. These w_2 and w_1
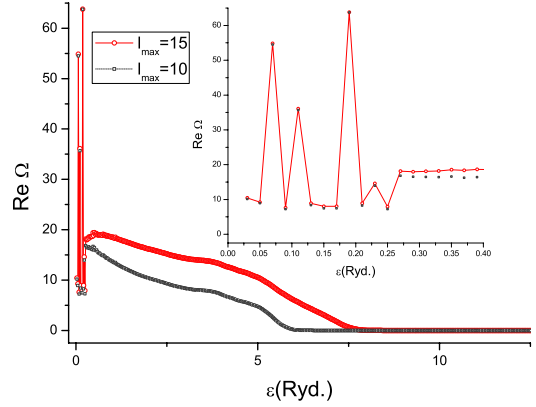

Fig. 1. Real part of the collision strength as a function of the colliding electron energy for two values of the maximum angular momentum l_{max}. Squares: $l_{max} = 10$. Circles: $l_{max} = 15$.

were calculated in an intermediate coupling framework by including the fine-structure effects and relativistic corrections resulting from breakdown of the LS coupling approximation for the target ions. A comparison between these calculations and experimental results has proven to be a good agreement for the first time for highly charged ions. The line widths w_c calculated by Ralchenko et al. (2001) with convergent close-coupling methods are also presented. These authors find (i) that calculated widths are generally smaller than both those measured and most of theoretical line widths from semiclassical calculations; and (ii) that the deviation between experiment and theory monotonically increases along the isoelectronic sequence, reaching a factor of 2 for Ne VII.

We performed calculations for each ion for the temperature values for which the experimental data are available. Principally, all the corresponding experimental results cited in the present work have been published by two groups. The first group (Blagojević et al. 1999, 2000) used a low-pressure pulsed arc and the second group (Wrubel et al. 1996, 1998) used a gas-liner pinch. The accuracy of the experimental line widths is generally given by Konjević et al. (2002) except for the few cases where other references have been mentioned. For 2s3s $^1S \leftarrow$ 2s3p ^1P transitions in F VI ions, we compared our results with w_1 of Elabidi et al. (2008) as there are no experimental results available yet.

To assess the quality of our calculations, we performed systematic comparisons with earlier experimental and theoretical data. Our results in Tables 1–7 agree well with both the experimental results and the previous theoretical calculations. Our results for the triplet transitions of N IV, for both the singlet and triplet transitions of O V, and singlet transitions of Ne VII are found to be in excellent agreement with the corresponding experimental results. However, the line widths for triplet transitions of Ne VII revealed a significant difference between our calculations and the corresponding measurements (see Table 6). Our calculated width of the transition line $^3S_1 \leftarrow {}^3P_1$ at vacuum wavelength 1992.06 Å is about 0.308 Å, while the corresponding measurement is about 0.45 Å and the difference amounts to 32%. We summarize our results by examining them in the following section by presenting line widths $W = 2w$ (*FWHM*) of singlet and triplet transitions 2s3s ← 2s3p in four Be-like ions from N IV to Ne VII:

Line widths of N IV. In Tables 1 and 2, we present our results for the line widths of singlet and triplet transitions 2s3s ← 2s3p

Table 1. Electron-impact widths W (FWHM) for the N IV 2s3s ^{3}S $\leftarrow$ 2s3p ^{3}P transitions at various electron temperatures T_e and electron densities N_e.

N IV Transition	T_e (10^4 K)	N_e (10^{17} cm^{-3})	W (Å)	w_1 (Å)	w_2 (Å)	w_m (Å)	w_c (Å)
^{3}S$_1$ $\leftarrow$ ^{3}P$_2$	5.4	2.8	0.400	0.381	0.555	0.410^c	0.246
(3478.72 Å)	7.24	0.86	0.110	0.116	0.170	0.122^a	0.070
	7.83	0.99	0.122	0.132	0.194	0.136^a	0.080
	8.01	1.13	0.138	0.151	0.221	0.148^a	0.090
	8.07	1.21	0.147	0.161	0.237	0.153^a	0.094
	8.12	5.80	0.703	0.773	1.13	0.84^b	0.452
	8.23	1.33	0.160	0.177	0.26	0.172^a	0.102
	9.63	8.1	0.909	1.06	1.55	1.11^b	0.613
	9.86	15.8	1.75	2.05	3.02	1.46^b	1.168
	10.1	19.4	2.213	2.51	3.69	1.72^b	1.421
	10.44	10.6	1.15	1.36	2.01	1.11^b	0.776
^{3}S$_1$ $\leftarrow$ ^{3}P$_1$	5.4	2.8	0.403	0.383	0.564	0.330^c	0.246
(3483.00 Å)	7.24	0.86	0.110	0.117	0.172	0.122^a	0.070
	7.83	099	0.123	0.133	0.197	0.136^a	0.080
	8.01	1.13	0.139	0.152	0.225	0.150^a	0.090
	8.07	1.21	0.148	0.163	0.240	0.150^a	0.095
	8.12	5.8	0.708	0.778	1.15	0.84^b	0.449
	8.23	1.33	0.161	0.178	0.264	0.174	0.102
	9.63	8.1	0.916	1.06	1.58	1.10^b	0.604
	9.86	15.8	1.77	2.08	3.07	1.46^b	1.168
	10.1	19.4	2.15	2.53	3.75	1.72^b	1.433
	10.44	10.6	1.15	1.38	2.04	1.11^b	0.776
^{3}S$_1$ $\leftarrow$ ^{3}P$_0$	5.4	2.8	0.400	0.385	0.571	0.400^c	0.245
(3484.93 Å)	7.24	0.86	0.110	0.117	0.174	0.122^a	0.070
	7.83	0.99	0.122	0.134	0.199	0.146^a	0.080
	8.01	1.13	0.138	0.153	0.227	0.146^a	0.090
	8.07	1.21	0.147				
	8.12	5.8	0.705	0.782	1.16	0.84^b	0.454
	8.23	1.33	0.161				
	9.63	8.1	0.912	1.07	1.59	1.10^b	0.601
	9.86	15.8	1.76	2.08	3.09	1.46^b	1.159
	10.1	19.4	2.14	2.54	3.78	1.72^b	1.433
	10.44	10.6	1.15	1.38	2.06	1.11^b	0.776

Notes. Vacuum wavelengths given in parentheses for each transition, W presents calculations, w_2 full quantum mechanical calculations, w_1 simplified calculations of Elabidi et al. (2008), w_m experimental widths, w_c the quantum calculations of Ralchenko et al. (2001) (same notations in the following tables); $^{(a)}$, $^{(b)}$, and $^{(c)}$ represent for experiments Blagojević et al. (1999), Wrubel et al. (1998), and Milosavljević & Djeniže (1998), respectively.

Table 2. Electron-impact widths W (FWHM) for 2s3s ^{1}S$_1$ $\leftarrow$ 2s3p ^{1}P$_1$ transitions of N IV, where the line widths are listed as a function of electron temperature T_e under electron density $N_e = 10^{18}$ cm^{-3}.

N IV Transition	T_e (10^4 K)	W (Å)	w_1 (Å)	w_2 (Å)	w_m (Å)	w_c (Å)
^{1}S$_0$ $\leftarrow$ ^{1}P$_1$	2.320890	4.80	4.41	6.27		
(6380.75 Å)	4.641779	3.47	4.55	6.59		
	6.962669	2.77	4.46	6.49		
	7.190000	2.72	4.45	6.46	3.89	2.82
	8.120000	2.53	4.37	6.37	3.76	2.72
	9.283559	2.34	4.27	6.24		
	11.60445	2.04	4.07	5.95		
	13.92534	1.81	3.87	5.66		
	16.24623	1.63	3.69	5.40		
	18.56712	1.49	3.51	5.15		
	20.88801	1.37	3.37	4.94		
	23.20890	1.27	3.23	4.74		

Notes. Experimental widths w_m are cited from Wrubel et al. (1998).

Table 3. Electron-impact widths W (FWHM) for the O V 2s3s ^{3}S $\leftarrow$ 2s3p ^{3}P transitions.

O V Transition	T_e $(10^4$ K)	N_e $(10^{17}$ cm$^{-3})$	W (Å)	w_1 (Å)	w_2 (Å)	w_m (Å)	w_c (Å)
^{3}S$_1 \leftarrow ^3$P$_1$	5.46	0.95	0.0573	0.054	0.079	0.077	0.0360
(2786.99 Å)	6.19	1.38	0.0807	0.079	0.116	0.102	0.051
	6.55	1.09	0.0628	0.062	0.092	0.073	0.0399
	7.97	1.41	0.0764	0.080	0.118	0.100	0.050
	8.87	1.57	0.0820	0.088	0.131	0.105	0.0541
	9.16	1.68	0.0867	0.094	0.140	0.102	0.0570
	9.33	1.54	0.0790	0.086	0.128	0.105	0.0530
^{3}S$_1 \leftarrow ^3$P$_0$	6.19	1.38	0.0819	0.079	0.117	0.098	0.0510
(3484.93 Å)	7.97	1.42	0.0780	0.081	0.121	0.098	0.050
	8.87	1.57	0.0830	0.088	0.133	0.105	0.0541
	9.16	1.68	0.0878	0.094	0.142	0.108	0.0571

Notes. w_m from Blagojević et al. (1999).

Table 4. Electron-impact widths W (FWHM) for the O V 2s3s ^{1}S $\leftarrow$ 2s3p ^{1}P transitions.

O V Transition	T_e $(10^4$ K)	N_e $(10^{17}$ cm$^{-3})$	W (Å)	w_1 (Å)	w_2 (Å)	w_m (Å)	w_c (Å)
^{1}S$_1 \leftarrow ^1$P$_1$	9.05	10.8	2.22	1.94	2.89	1.85	1.12
(5114.06 Å)	10.8	12.0	2.25	2.10	3.13	2.01	1.21
	16.7	17.2	2.54	2.74	4.08	2.16	1.57
	21.7	23.6	2.97	3.48	5.16	2.85	2.04

Notes. w_m from Wrubel et al. (1998).

Table 5. Electron-impact widths W (FWHM) for the F VI 2s3s ^{1}S $\leftarrow$ 2s3p ^{1}P transitions listed as a function of electron temperature T_e under electron density $N_e = 10^{18}$ cm^{-3}.

F VI 2s3s ^{1}S$_0 \leftarrow$ 2s3p ^{1}P$_1$ (6830.75 Å) $N_e = 10^{18}$ cm^{-3}		
T_e $(10^4$ K)	W (Å)	w_1 (Å)
2.320890	10.376	0.757
4.641779	5.981	0.869
6.962669	4.318	0.889
9.283559	3.441	0.881
11.60445	2.893	0.861
13.92534	2.514	0.836
16.24623	2.235	0.810
18.56712	2.019	0.782
20.88801	1.846	0.757
23.20890	1.704	0.734

of N IV ion for various electron temperatures and densities along with the experimental results (Blagojević et al. 1999, 2000; Wrubel et al. 1996, 1998). The previous theoretical calculations w_c of Ralchenko et al. 2001), the full quantum mechanical calculations w_2 and its simplified calculations w_1 of Elabidi et al. (2008) are also listed in Tables 1 and 2. The experimental measurements w_m give singlet and triplet transitions 2s3s $\leftarrow$ 2s3p line widths of N IV ions at different electron temperatures. The measurements by Milosavljević & Djenize (1998) were carried out for electron temperature $T_e = 5.4 \times 10^4$ K, while Blagojević et al. (1999) considered some lower temperatures, and Wrubel et al. (1998) measured at higher temperatures. From Table 1, our results are in good agreement with the experimental values. In detail, most of

the other spectral line widths are in good agreement with w_m within 5%. The difference for the majority of the spectral lines amounts to 10% and the most significant difference reaches to 18%. Additionally, there are a few cases where the difference between our results and existing experimental values is large. For example, in the transition ^{3}S$_1 \leftarrow ^3$P$_2$ under plasma condition $T_e = 9.63 \times 10^4$ K and $N_e = 8.1 \times 10^{17}$ cm^{-3}, the difference in the line width reaches to 18%. Similarly, the transitions ^{3}S$_1 \leftarrow ^3$P$_1$ and ^{3}S$_1 \leftarrow ^3$P$_0$ in Table 1 have two and four exceptional cases, respectively, which our results show as large deviations from experimental values. For singlet transitions listed in Table 2, it can be seen that the discrepancies between W and two experimental results w_m cited by Bochum Group (Wrubel et al. 1996, 1998) are within 33%. Our results are less than experimental w_m in contrast to w_1. When compared with w_m, our results are better than w_2, but worse than w_1. Overall, our results W for triplet transitions are always better than those of singlet transitions.

Line widths of O V. In Tables 3 and 4, we compare our theoretical calculations of line widths for the singlet and triplet transitions 2s3s $\leftarrow$ 2s3p of O V ion for various electron temperatures and densities. We also note that the measured widths are determined with an error of 23%: the error of the temperature determination is 18−27% and 15% for the density determination (Elabidi et al. 2008). In triplet transitions in O V, our results are consistent with w_1 and agree with each other, but w_2 are closer to the experimental values when compared to our calculations. However, in singlet transitions, w_1 is the best in two first lines of the table, and our results are the best in two last lines, while w_2 is the worst. Most of our line width results are within an error of 15%, and the maximum error is about 25% in comparison to the experimental results.

Line widths of F VI. In Table 5, we list our results W as a function of electron temperature under an electron density

Table 6. Electron-impact widths W (FWHM) for the Ne VII 2s3s ^{3}S $\leftarrow$ 2s3p ^{3}P transitions under electron density of $N_e = 3 \times 10^{18}$ cm^{-3}.

Ne VII Transition (Å)	$T_e = 2.38 \times 10^5$ K W (Å)	w_1 (Å)	$N_e = 3 \times 10^{18}$ cm^{-3} w_m (Å)	w_c (Å)
^{3}S$_1 \leftarrow$ ^{3}P$_2$(1981.97 Å)	0.309	0.378	0.45^a	0.230
^{3}S$_1 \leftarrow$ ^{3}P$_1$(1992.06 Å)	0.308	0.383	0.45^b	0.230
^{3}S$_1 \leftarrow$ ^{3}P$_0$(1997.35 Å)	0.309	0.391	0.45^a	0.230

Notes. $^{(a)}$ and $^{(b)}$ selected from Wrubel et al. (1996) and Wrubel et al. (1998) respectively; w_c: the results of Ralchenko et al. (1999).

Table 7. Electron-impact widths W (FWHM) for the Ne VII 2s3s ^{1}S $\leftarrow$ 2s3p ^{1}P transitions under electron density of $N_e = 3.5 \times 10^{18}$ cm^{-3} and electron temperature $T_e = 2.205 \times 10^5$ K.

Ne VII Transition (Å)	$T_e = 2.205 \times 10^5$ K W (Å)	w_1 (Å)	w_2 (Å)	$N_e = 3.5 \times 10^{18}$ cm^{-3} w_m (Å)	w_c (Å)
^{1}S$_0 \leftarrow$ ^{1}P$_1$ (3643.60 Å)	1.32	1.17	1.5	1.70	1.00

Notes. The experimental result is selected from Wrubel et al. (1998), and w_c is result of Ralchenko et al. (1999).

$N_e = 10^{18}$ cm^{-3}. There are no experimental results available for F VI ^{1}S$_0 \leftarrow$ ^{1}P$_1^\circ$ line widths. Only the quantum mechanical calculations w_1 of Elabidi et al. (2008) are listed in Table 5 for comparison purposes. Our calculations show large differences from w_1 results. Regarding this discrepancy between the quantum mechanical calculation w_1 and our theoretical calculations, the reader may wonder about the cause of such a difference. At present, we cannot understand this discrepancy. The reasons of this discrepancy need to be investigated both experimentally and theoretically in future.

Line widths of Ne VII. In Table 6, we report our results for the triplet transitions of Ne VII along with the experimental line widths measured by the Bochum group (Wrubel et al. 1996, 1998) at electron density $N_e = 3 \times 10^{18}$ cm^{-3} and electron temperature $T_e = 2.38 \times 10^5$ K. A comparison between our results and the measurements yields a maximum difference of 32%. Our results are in good agreement with the theoretical calculations w_1.

In Table 7, we present the line widths for singlet transition of Ne VII ion at electron density $N_e = 3.5 \times 10^{18}$ cm^{-3} and electron temperature $T_e = 2.205 \times 10^5$ K. A comparison between W and w_m (Wrubel et al. 1998) shows that the difference is within 22%. It indicates that our results W for line widths of Ne VII are in good agreement with w_m and are more accurate than w_1 but less accurate than w_2.

5. Conclusions

In the present work, a new set of electron-impact broadening of the singlet and triplet transition 2s3s $\leftarrow$ 2s3p in four Be-like ions from N IV to Ne VII have been obtained by solving the ($N + 1$)-electron colliding systems of Be-like ions with DARC on the basis of relativistic quantum mechanical approach. Spectral line widths of triplet transitions of N IV ion are in best agreement with experimental values. A maximum discrepancy of 32% appears between W and w_m for triplet transitions of Ne VII ion at electron density $N_e = 3 \times 10^{18}$ cm^{-3} and electron

temperature $T_e = 2.38 \times 10^5$ K, which can be considered as tolerable agreement with respect to the accuracy of the experiment. Overall, one can conclude that our results for all defined temperatures agree with the experimental values within 10%, 20%, and 30% for N IV, O V, and Ne VII respectively. For singlet transitions in F VI ion (see Table 5), our results are quite different from w_1, which needs clarification in future studies. Our calculations further support the argument of good agreement between quantum mechanical calculations and experiments for line widths of $\triangle n = 0$ transitions in highly charged ions in accordance with the conclusion of Elabidi et al. (2008). Our present calculations will be used for plasma diagnostics.

References

Baranger, M. 1958a, Phys. Rev., 111, 481
Baranger, M. 1958b, Phys. Rev., 111, 494
Baranger, M. 1958c, Phys. Rev., 112, 855
Bari, M. A., Salahuddin, M., Duan, B., Nasim, M. H., & Hussain, S. A. 2011, J. Phys. B, 44, 225004
Berrington, K. A., Burke, P. G., Dufton, P. L., & Kington, A. E. 1977, J. Phys. B, 8, 1465
Blagojević, B., Popović, M. V., Konjević, N., & Dimitrijević, M. S. 1999, J. Quant. Spectr. Radiat. Trans., 61, 361
Blagojević, B., Popović, M. V., & Konjević, N. 2000, J. Quant. Spectr. Radiat. Trans., 67, 9
Dimitrijević, M. S., & Konjević, N. 1980, J. Quant. Spectr. Radiat. Trans., 24, 451
Duan, B., Bari, M. A., Zhong, J. Y., et al. 2008, A&A, 488, 1155
Dyall, K. G., Grant, I. P., Johnson, C. T., Parpia, F. A., & Plummer, E. P. 1989, Comput. Phys. Commun., 55, 425
Elabidi, H., Ben Nessib, N., & Sahal-Bréchot, S. 2004, J. Phys. B, 37, 63
Elabidi, H., Ben Nessib, N., Cornille, M., Dubau, J., & Sahal-Bréchot, S. 2008, J. Phys. B, 41, 025702
Griem, H. R. 1974, Spectral Line Broadening by Plasma (NewYork, USA: Academic press)
Hooper, C. F. Jr. 1966, Phys. Rev., 149, 77
Konjević, N., Lesage, A., Fuhr, J. R., & Wiese, W. L. 2002, J. Phys. Chem. Ref. Data, 31, 819
Milosavljević, V., & Djenize, S. 1998, A&AS, 128, 179
Norrington, P. 2009, DARC manual, http://www.am.qub.ac.uk/users/p.norrington
Ralchenko, Y., Griem, H. R., Bray, I., & Fursa, D. V. 1999, Phys. Rev. A, 59, 1890
Ralchenko, Y., Griem, H. R., Bray, I., & Fursa, D. V. 2001, J. Quant. Spectr. Radiat. Trans., 71, 595
Seaton, M. J. 1987, J. Phys. B, 20, 6431
Parpia, F. A., Froese Fischer, C., & Grant, I. P. 1996, Comput. Phys. Commun., 94, 249
Peach, G. 1996, in Atomic, Molecular & Optical Physics Handbook, ed. G. W. F. Drake (New York: AIP Press), 669
Wrubel, Th., Glenzer, S., Bücher, S., Kunze, H. J., & Alexiou, S. 1996, A&A, 307, 1023
Wrubel, Th., Ahmad, I., Bücher, S., Kunze, H. J., & Glenzer, S. 1998, Phys. Rev. E, 57, 5972